A new phase-correlation-based Iris matching for degraded images

Emine Krichen, Sonia Garcia-Salicetti, Bernadette Dorizzi

A New Phase Correlation-based Iris Matching for Degraded Images

Emine Krichen, Sonia Garcia-Salicetti and Bernadette Dorizzi

Institut TELECOM; TELECOM & Management SudParis; Equipe Intermedia

Abstract*—In this paper, we present a new phase correlation-based iris matching approach in order to deal with degradations in iris images due to unconstrained acquisition procedures. Our matching system is a fusion of global and local Gabor phase correlation schemes. The main originality of our local approach is that we do not only consider the correlation peak amplitudes but also their locations in different regions of the images. Results on several degraded databases namely CASIA-BIOSECURE and Iris Challenge Evaluation 2005 databases, show the improvement of our method compared to two available Reference Systems, MASEK and OSIRIS, in verification mode.

***Index Terms*—Iris verification, local and global correlation-based method, degraded iris images, Gabor phase**

I. INTRODUCTION

Iris shows high richness in pattern and it is the only internal organ which is externally visible. While its acquisition was highly constrained up to recently, it can be imaged, at least theoretically, from a very comfortable distance for the user by using machine vision technology [1]. It doesn't suffer from day to day changes (time variability) and it is an epigenetic pattern, a useful trait to discriminate individuals that are genetically related like twins [2]. For these reasons, iris is an interesting biometric modality for verifying and even identifying an individual. Indeed, John Daugman proposed the first successful algorithm for iris recognition [3] [4], which is running in most commercial iris recognition systems.

Daugman's system is based on two major and original achievements: on one hand, the use of 2-D Gabor filters as carrier waves to extract only phase information; on the other hand, the use of Bernoulli trials to fit the inter-class distribution after phase quantization. Daugman proved with an appropriate metric that the inter-class

distribution is stable with respect to database sizes [5]. This corresponds to a remarkable achievement in biometrics.

More precisely, Daugman used a 2D complex Gabor wavelet filter at different scales and different positions spanning three octaves. Based on Oppenheim and Lim's work [6] that demonstrated the importance of phase for texture characterization, Daugman used a phase quantization method following the four quadrant principle, to extract an iris code from the filtered iris images. Other authors derive the codes using zero-crossing methods [7]. To compare codes, Daugman used as metric the Hamming distance. Then, in order to find an optimal decision threshold, he interpolated the inter-class distribution, that could be supposed to be a normal distribution thanks to the Bernoulli trials technique. Finally, he showed on different large size databases that the empirical inter-class distribution and the fitted inter-class distribution (normal) coincide [2] [3] [5].

This system has been tested intensively through all these years [8]. What emerges from such years of research and benchmarking is that iris is a high accurate biometric modality in terms of performance on clean iris images acquired in a very constrained scenario. More recently, the research community has started investigating how iris recognition systems react to less constrained acquisition conditions, resulting in degraded iris images (blurring, iris mostly occluded by eyelids and eyelashes, iris acquired under eyeglasses, from varying distances, with a standard camera …).

The National Institute of Standards and Technology (NIST) organized in 2005 the Iris Challenge Evaluation (ICE), aiming at measuring and comparing state-of-the-art iris recognition performance on realistic environments, therefore leading to improvements in iris recognition research and development [9]. The iris data was captured by the LG2200 camera, resulting in 2953 images from 132 subjects. Although some quality control was applied during data collection, some "non-ideal" iris images are still present in the database, such as occlusion by eyelids and eyelashes, defocus, off-angle images and motion blur. The first report on this competition shows a FRR varying from 30% (worst case) to around 0.2% for the best system, at 0.1% of FAR. Globally, 5 systems among 13 show a low FRR, below 0.7% at 0.1% of FAR [10]. More recently, a second report describes results on an extended version of the database, called ICE 2006, containing 59558 images of 240 persons [11], including very degraded images: off-angle images, blurred images with highly dilated pupil, highly covered images by eyelids, iris images taken with patterned contact lenses. This report shows a degradation of systems' performance in general. Indeed, in ICE 2006 the FRR varies from 0.5% to 4% at 0.1% of FAR, whereas, for the best systems, it varied from 0.1% to 0.7% at 0.1% of FAR in ICE 2005.

Alongside ICE database, the CASIAv2 database is well-known in the research community as a publicly available set of degraded images, containing strong eyelids and eyelashes occlusions, and different illuminations [12]. Also, the University of West Virginia built a private database of non ideal iris images and studied the robustness of their own version of Daugman's algorithm on such data [13]. Results show substantial degradation in performance when iris images are low textured and highly occluded. Chen [14] also used the West Virginia database and their own version of Daugman's system to measure how the quality of iris data affects the algorithm. To that end, they split the database into five different sets labelled from "Very poor image quality" to "Very good image quality", and show the degradation of performance from one set to another. On the same database, Schukers and al. [15] proposed to estimate and correct the off-angle effects on the iris images. They used an angular calibration model and Daugman's integrodifferential operator to that purpose and showed an improvement in performance on two different recognition methods based respectively on global Independent Component Analysis (ICA) and biorthogonal wavelets. To handle non ideal iris images, J. Daugman proposes a quality measure calculated as a function of several measures including percentage of visible iris, blur measures using the Fourier transform and the sharpness of the pupil boundary and interlaced raster shear detection [16]. Daugman shows a strong correlation between the Hamming distances and the quality of the images, of the intraclass comparisons. This can be used to set up more reliable quality-dependent decision thresholds.

In this paper, we propose an alternative method based on phase correlation, specially designed to cope with degraded iris images. Wildes was the first to propose to match irises by a correlation measure on four resolutions after applying Laplacian filters [17]. Scores produced at each resolution were fused by Fisher analysis. Since then, several works have explored correlation measures.

Kumar et al. [18] proposed new techniques on correlation filter design in frequency space. They adapted their method to biometrics and especially to face and iris. A filter is designed for each iris class using several images at the learning stage. The test image is correlated with the filter designed previously instead of being correlated to the reference image or a set of reference images, as in a classical implementation of a correlation-based system.

Miyazawa et al. [19] introduced a phase correlation-based method for iris in the frequency domain using Fourier phase information. They introduced the principle of a "Band Limited Phase Only Correlation" that consists in detecting pertinent frequencies for iris matching.

Our method is original regarding to these three systems in different respects. First, we exploit the complementarity of local and global correlation measures, and second, at the local level, we use in addition to

the peak amplitude, the information conveyed by the position of such peak. Like Wildes, we used local correlation techniques but our filtering step is based on Gabor filters which bring more information from the iris image than grey-level or Laplacian filters. Like Miyazawa, we have used a phase correlation technique but we have computed wavelet coefficients instead of Fourier coefficients. This allows us to precisely use local correlation measures while keeping the relation between the extracted features in frequency space and local position in the iris image; indeed, this is impossible in the Fourier domain where position information in the original domain is lost.

In the next section, we describe all the modules of our phase correlation-based system, including iris segmentation and normalization, phase extraction, modified normalized correlation method and fusion strategies. In the third section, we introduce the databases on which we have run the experiments. In these experiments, we have used ICE 2005 database, CASIAv2 database, and the CASIA-BIOSECURE data set (CBS); CBS database results from merging CASIAv2 with new data acquired with the same protocol and the same sensors as CASIAv2, in the framework of the European Network of Excellence BioSecure [20]. Also, as benchmarking tools for our system, we consider two iris reference systems, MASEK [21] (used by NIST) and OSIRIS [22], a new reference system developed by our team in the framework of BioSecure. Finally, conclusion and future work will be discussed.

II. IRIS RECOGNITION SYSTEM

A. Iris Segmentation and Normalization

The first step of any iris recognition system is locating the iris rim defined by the pupil and iris boundaries. We have used for that purpose a well-known state-of-the-art method based on the Hough Transform. All algorithms mentioned later in this article have used the same segmentation module which has been developed by Masek and modified and optimised by our team. Note that this segmentation method is not adequate for degraded images and that recent works use Active Contour Approaches [4]. However, as we want to show the robustness of correlation approaches to degradations, we will use a Hough-based segmentation algorithm. An iris rim may show different sizes depending on the dilation or contraction of the pupil and the relative position between the camera and the person. In order to normalize the iris images, we have used the rubber sheet model normalization proposed in [3]. The Cartesian representation of an iris image is transformed into a fixed size rectangular representation, in which the angular information is represented in the row of the image and radial

information is represented in the column. We used in our experiments a normalized image size of 80x512 pixels. We performed an adaptive histogram equalisation to the normalised images. The segmentation and normalization process are shown in Figure 1. No eyelids and eyelashes detection were performed.

B. Gabor Phase Extraction: motivation

A general weakness of correlation approaches is their intolerance to illumination variations. Indeed, when strong illumination is present, high correlation peak amplitude may be observed between iris images of different persons, and the other way round, when there is weak texture energy (dark images) in the image, the correlation peak amplitude may be attenuated even between irises from the same person. One way to cope with this problem is to normalize each image with respect to its texture energy, but this only solves the difficulty partially. This problem does not exist if the phase-based approach is adopted: given an iris image $I(x,y)$ corrupted by uniform illumination which is modeled by a multiplicative factor A and thus transformed into another image $J(x,y) = A*I(x,y)$, if the Transform of I is $T(I)$, then the Gabor Transform of J is $T(J) = A*T(I)$. Therefore, when comparing I to J (represented by their transformed image in frequency space $T(I)$ and $T(J)$), the real and imaginary parts as well as the amplitude of the Gabor transform of J are still corrupted by factor A, whereas the phase of $T(I)$ is equal to the phase of $T(J)$. Of course, illumination effects on grey-level images are rarely uniform across a whole image, but even if illumination depends on pixel position, phase information resists better to illumination variations [6].

Although both Fourier and Gabor phases have the same property, Fourier analysis does not offer the possibility of relating spatial information (pixel position) to the phase value extracted. Also, Gabor analysis allows to extract information at different resolutions and orientations [23]. Samples of Gabor phase images for a given iris image are shown in Figure 2, spanning several resolutions and orientations.

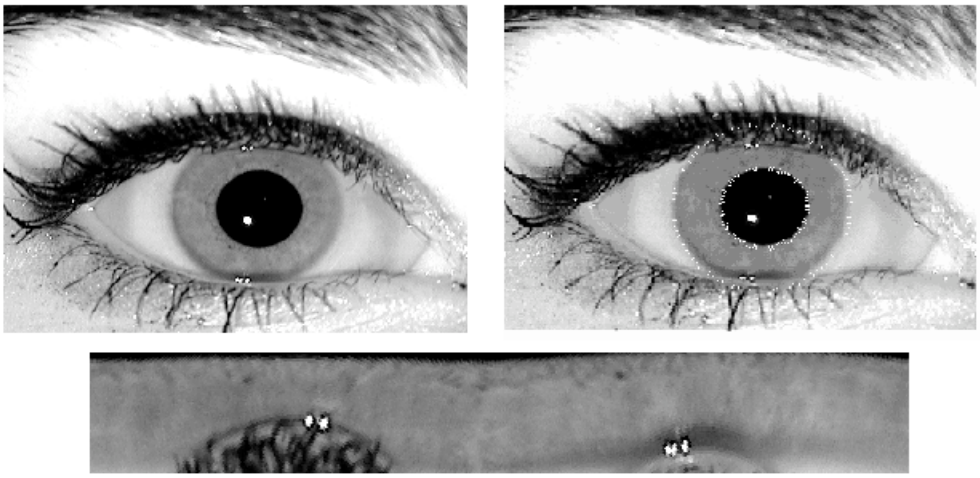

Fig1. Original iris image from ICE database (top left), Segmented iris (top right) and unwrapped form

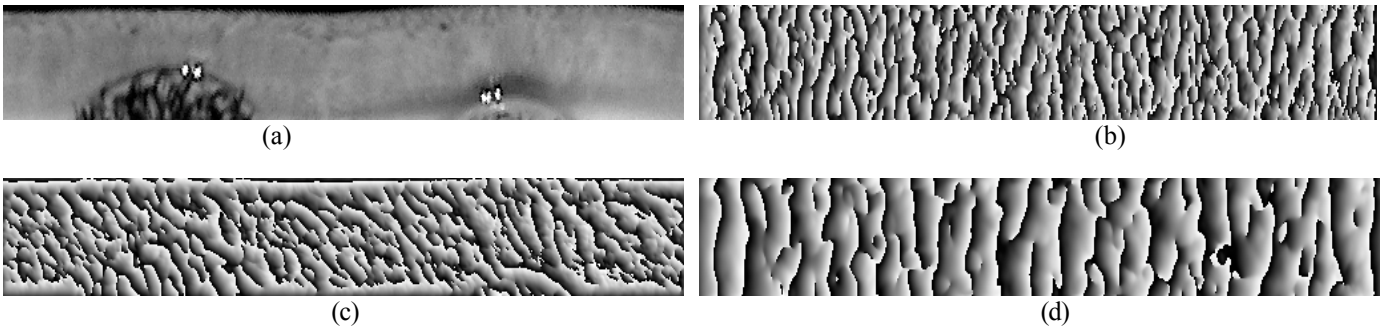

Fig2. Iris Gabor phase images spanning several scales and orientations: (a) original normalized image; (b) first resolution, vertical orientation; (c) first resolution, diagonal orientation; (d) second resolution, vertical orientation.

C. Normalized Phase Correlation

In our work, because of the intolerance of standard correlation to illumination variations, we consider the normalized cross-correlation measure proposed in [24], given at pixel *(u,v)* by:

$$C(u,v) = \frac{\sum_{x,y}[I(x,y) - \bar{I}_{u,v}][J(x-u,y-v) - \bar{J}]}{\sum_{x,y}[I(x,y) - \bar{I}_{u,v}]^2 \sum_{x,y}[J(x-u,y-v) - \bar{J}]^2} \qquad (1)$$

where I is the reference image, J the test image (that may be of a smaller or equal size) positioned at pixel (u,v) of I, $\bar{J}$ is the mean of J and $\bar{I}_{u,v}$ is the mean of I in a neighbourhood of pixel (u,v) of size equal to that of J. If I and J belong to the same person, $Max_{u,v}\, C(u,v)$ is equal or close to 1. Then, we consider as measure of the peak amplitude the "Peak to Slob Ratio" (PSR) [18] which takes into account the mean value of the correlation matrix C and its standard deviation by the equation given in the following:

$$PSR = \frac{Max(C) - Mean(C)}{STD(C)} \qquad (2)$$

In the following, we study two approaches: one in which correlation is applied globally on the image ("global correlation-based method"), and one in which correlation is applied to regions of the image ("local correlation-based method"). We denote as *I* the reference image and as *J* the test image. Of course, *I* and *J* are phase images at a given filter resolution and orientation.

1) Local correlation-based method: One of the most difficult variability to handle in iris recognition is due to rotations. As explained previously, the iris rim is transformed into a normalized rectangular shape, in which rotations are transformed into translations in the horizontal direction. On the other hand, the non linear stretch of iris texture due to pupil's dilation or contraction cannot be perfectly handled by a linear normalization process, and thus a change is generated in the normalized image in the vertical direction as well. In the literature, only the peak amplitude is used for matching, whereas we propose in this work to also exploit the translation of such correlation peak. Indeed, when genuine irises are matched, the observed translations are constant, while random translations characterize impostures. Our method is designed to handle these problems by combining correlation peak amplitude and position standard deviations.

We have divided the test image *J* into several sub-images $\{J_W\}$, each of size *W*, and the reference image *I* into another set of sub-images $\{I_{W'}\}$ each of size $W'>W$ in order to be able to detect each test sub-image J_W in $I_{W'}$. This choice is motivated by the necessity of a bigger window in the reference image, to cope with rotations and pupil dilation and contraction after image unwrapping. Then, we correlate each J_W with its corresponding $I_{W'}$ and store both the magnitude of the correlation peak in terms of *PSR(W)* and peak position *PP(W)*. Finally, we compute the Local Similarity Score (*LSS)* between *I* and *J* as:

$$LSS(I,J) = \frac{Mean_W(PSR(W))}{Std_W(PP(W))} \qquad (3)$$

If *I* and *J* belong to the same person, a high *LSS(I,J)* may be observed since the peak amplitude should be high and the standard deviation should be small simultaneously. On the contrary, if *I* and *J* do not belong to the same person, the peak position may be observed anywhere in the correlation matrix and is independent from one sub-image to the next, thus presenting a high standard deviation. In this case, a lower *LSS(I,J)* should be obtained, compared to that observed when *I* and *J* belong to the same person.

2) Global correlation-based method: We have chosen to consider as test image *J* an image of a slightly lower size compared to that of the reference image *I*. We perform correlation between *I* and *J* in order to measure the

Global Similarity Score (*GSS(I,J)*), equal to the *PSR* defined in Equation (2). In this case, the peak position is not useful.

D. Fusion

In fact, fusion operates in our system at different levels; in each one, a different strategy has been employed.

In our experiments, we have used 4 resolution Gabor filters (10 pixels for the mother wavelet), and 4 orientations (0°, 45°, 90°, 135°) for each. This way, from one image, we extract 16 filtered images (some examples are shown in Figure 2), and for each comparison between two irises we have therefore 16 matches to perform.

We recall that I and J are unwrapped iris images, and $I_{R,\_}$ and $J_{R,\_}$ are respectively their corresponding phase images, for a fixed filter resolution R and an orientation $\_$. First, we fuse separately local scores $LSS(I_{R,\_},J_{R,\_})$ and global scores $GSS(I_{R,\_},J_{R,\_})$ at each resolution level R by computing the mean values:

$$LSS_R(I,J) = \frac{\sum_{\theta} LSS(I_{R,\theta},J_{R,\theta})}{4} \qquad (4)$$

$$GSS_R(I,J) = \frac{\sum_{\theta} GSS(I_{R,\theta},J_{R,\theta})}{4} \qquad (5).$$

Then, at this stage, we have obtained 4 scores, one per resolution, of local and global types.

To combine these scores, a previous normalization process is required. Indeed, the images across resolutions are of different aspects (thin edges at low resolutions, coarse ones at higher resolutions), as can be seen in Figure 2. Consequently, at a high resolution, the mean values of the correlation scores will be higher than at a low resolution. We thus apply to each local and global score a Z-norm normalization by considering the mean and variance of the inter-class score distribution at resolution level R, as follows:

$$LSS(I,J) = \sum_R \frac{LSS_R - \mu_R}{\sigma_R} \qquad (6)$$

$$GSS(I,J) = \sum_R \frac{GSS_R - \mu_R}{\sigma_R} \qquad (7).$$

Finally, we average the two scores in order to define the Similarity Measure Score *SMS(I,J)* between I and J :

$$SMS(I,J) = \frac{LSS(I,J) + GSS(I,J)}{2} \qquad (8).$$

III. SYSTEMS EVALUATION ON DEGRADED IRIS DATA

A. Degraded databases

We have conducted our experiments on two reference near infrared databases containing degraded iris images that have become available, ICE 2005 [9] and CASIAv2 [12] data sets; we have also used a third database, CASIA-BIOSECURE (CBS), described in detail below.

The CASIAv2 data set is more challenging in terms of illumination changes, blurred images and eyelids/eyelashes occlusions than the original CASIAv1 database. It contains 30 persons, 2 eyes per person, 20 images per eye and 2 devices were used in the acquisition stage: OKI handheld commercial device and PATTEK, an iris capture device made by CASIA. In order to expand this database in number of persons and also to build a database containing both Chinese and European subjects in balanced proportion, we conducted in collaboration with CASIA another acquisition campaign in Europe. This acquisition followed the same protocol and was carried out with the same sensors as CASIAv2. A subset of 30 european persons, called BIOSECURE v1 was acquired. Finally, after mixing CASIA v2 and BIOSECURE v1, we obtained the CASIA-BIOSECURE database (CBS), of 60 persons, half Chinese half European, 2 eyes per subject, a with a rather strong intraclass variability including illumination, glasses effects (reflections), eyelids/eyelashes occlusion, blurred and noisy images. Alongside this database (CBS), we have used the ICE 2005 database used by the NIST in their Iris Challenge Evaluation 2005. This database contains 132 persons and for 112 of such persons, the two eyes have been acquired. ICE 2005 database contains a total number of 2953 images. The images were acquired using a LG 2200 device. Images include acquisition and motion blurred images, strong eyelids and eyelashes occlusions (few cases), and off-angle images.

B. Reference Systems for comparative experiments

For comparative purposes, we have used some available Open-source Reference Systems: the MASEK and OSIRIS Systems, detailed below.

1) Masek System: Libor Masek [21] from *The University of Western Australia* has developed a modular and Open-source iris recognition system running in Matlab. The system has three modules corresponding to the three stages of any iris recognition process, namely: segmentation, normalisation and classification. The classification process relies on the use of Log-Gabor filters and four quadrant phase encoder on 1D signal,

corresponding to one orientation on the iris rim. This system, mostly related to Daugman's work, offers a good benchmarking system for the community. The NIST has re-written the MASEK System in C language and used it as benchmarking algorithm for the Iris Challenge Evaluation.

2) OSIRIS System: OSIRIS ("Open Source for Iris") [22] is an Open source iris recognition system developed in the framework of the BioSecure Network of Excellence. The system is designed to be modular and implements Daugman's approach. The classification module is based on Gabor Phase demodulation and Hamming distance.

C. Benchmarking Protocols

We have used on ICE 2005 database the protocol of Experiment 1 (comparison of right iris images). It includes 8376 intraclass comparisons and 659.365 interclass comparisons [9]. Besides, we define in the following a test protocol on CBS database (60 persons). This protocol is designed to evaluate the algorithms robustness to whether persons are wearing glasses or not, to illumination variation during acquisition, to rotations, to eyelids and eyelashes occlusions. As the database contains 20 images per person, and the 10 first images (Set1) and 10 last images (Set2) are acquired under different illumination conditions, we propose the following protocol:

- for each device (OKI and PATTEK), we define two different experiments.

In the first experiment, only one image is considered as client reference, and randomly selected from Set1. We repeat this experiment 3 times by sampling a different reference from Set1 in each case and we average error rates. In the second experiment, 3 images are also randomly selected from Set1, form the client template, and we take the best score from the 3 comparisons.

- concerning forgeries, for each person, we select randomly one impostor among the 59 remaining subjects and consider the 10 images of Set 2 as impostor accesses. This way, the impostor accesses correspond to different illumination conditions than those of client references.

In the following, we denote the two subsets of CBS database according to the sensor used as CBS_OKI and CBS_PAT, where OKI denotes the data subset acquired with the OKI device and PAT the subset acquired with the PATTEK device.

D. Results

1) Correlation experiments

In order to build the best system from the different possible alternatives proposed in Section II.C among which

those of Equations (6), (7) and (8), we carried out experiments on ICE 2005 database by considering:

- only the mean of local peak values (which can be considered as the "standard" correlation method), denoted by System A;
- only the standard deviation of local peak positions, denoted by System P;
- the combination of local peak values and their positions in the correlation measure, denoted by System COR1, corresponding to the LSS score of Equation (6);
- the global correlation peak method, denoted by System COR2, corresponding to the GSS score of Equation (7);
- the fusion of the global and local approaches, denoted by System CORR, corresponding to the SMS score of Equation (8).

Figure 3 shows a rather unexpected result. In the local approach, considering only peak locations performs better than considering only peak amplitudes, that is the standard correlation-based method. The error rate is indeed divided by more than a factor 2 at the EER functioning point. Using locally both information improves results based only on one information. Figure 4 shows that when both information (peak amplitude and its position) are taken into account in the local approach, results are quite similar to those of the global system. Finally, the fusion of the global and local approaches outperforms all the other methods.

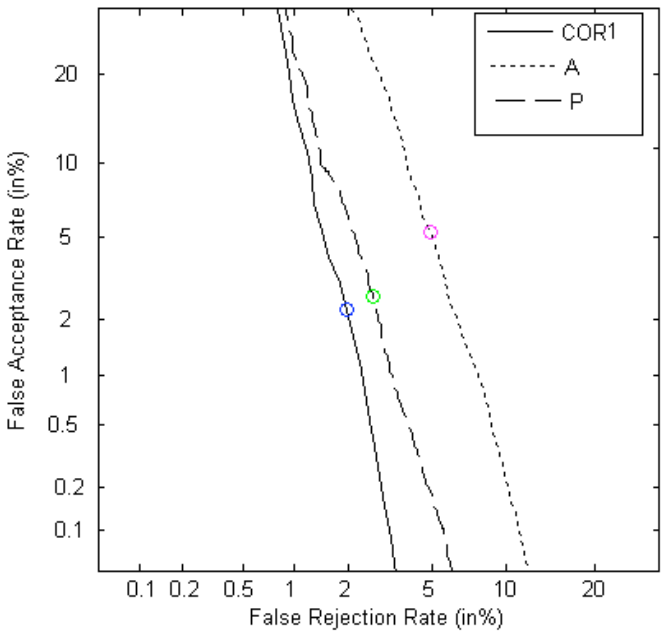

Fig.3 DET curves of different local Correlation-based systems: mean of local peak values (A- dotted curve), standard deviation of local peak positions (P- dashed curve), the combination of local peak values and their positions (COR1-solid curve). Bullets represent the EER functioning point.

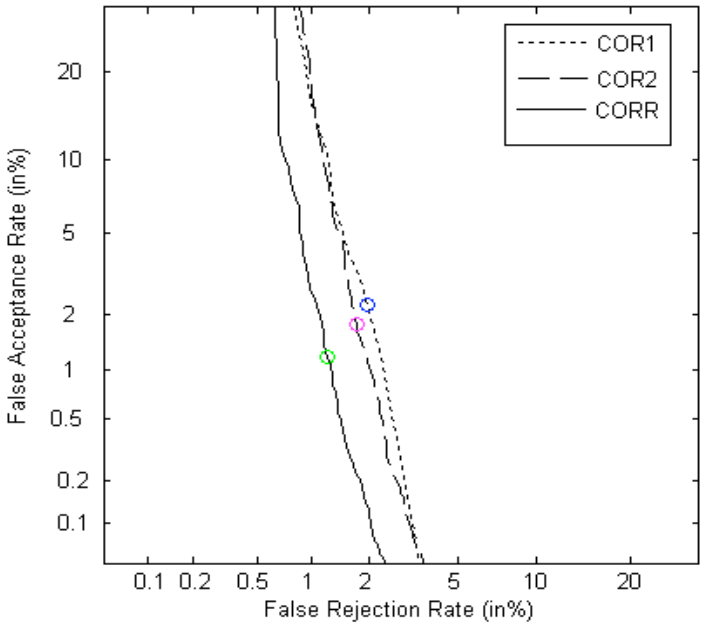

Fig.4 DET curves of different Correlation-based systems: global correlation method (COR2-dashed curve), the local correlation method (COR1-dotted curve) and finally the fusion of the local and global approaches (CORR-solid curve). Bullets represent the EER functioning point.

2) Comparative experiments

We performed experiments on two databases, ICE 2005 and CASIA-BIOSECURE that present interesting differences: for example CASIA-BIOSECURE database contains irises from Chinese and Western subjects in equal proportion, allows the presence of glasses and for this reason shows more reflections than ICE 2005; some challenging images are shown in Figure 12.

2.1 Comparative experiments on ICE 2005

2.1.1 Global comparative experiment

The first comparative experiment detailed in this paper is conducted on ICE 2005 database and follows the protocol of Experiment 1 (see Section III-C); it consists in comparing the proposed system fusing local and global correlation score (CORR) to OSIRIS and MASEK Reference Systems. Figure 5 shows that OSIRIS and CORR systems clearly outperform the MASEK system in the complete range of (FAR,FRR) values. Our system outperforms OSIRIS especially when high security functioning points are considered. In particular, for the 0.1%

of FAR functioning point, the gap in performance between the two systems is equal to 1% (2% of FRR for our system and 3% for OSIRIS).

Concerning results that have been reported in the literature on ICE 2005 database, it is not straightforward to compare recognition methods because systems are not benchmarked in equal conditions regarding the pre-processing and segmentation steps. For example, the same recognition methodology shows different FRR at 0.1% of FAR, varying from 0.1% to 0.7% depending on the pre-processing and segmentation used previously to recognition itself (case of Sagem-Iridian, Cambridge1 and Cambridge2 systems) [10]. Among them, some Correlation-based techniques reported performance on ICE 2005 which vary from 0.5% (Carnegie Mellon University) and more than 5% (Yamataki Corporation/Tohoku University) [10]. Our Correlation-based approach is globally well-ranked with 2% of FRR at 0.1% of FAR. We recall that no eyelids and eyelashes detections are performed prior to verification system and the only pre-processing used is adaptive histogram equalization on the normalized image. This has been done on purpose to show the robustness of the correlation approach to degradations. We then consider that our Correlation-based system is rather in an unfavourable position in this comparison, due to this lack of sophisticated pre-processing.

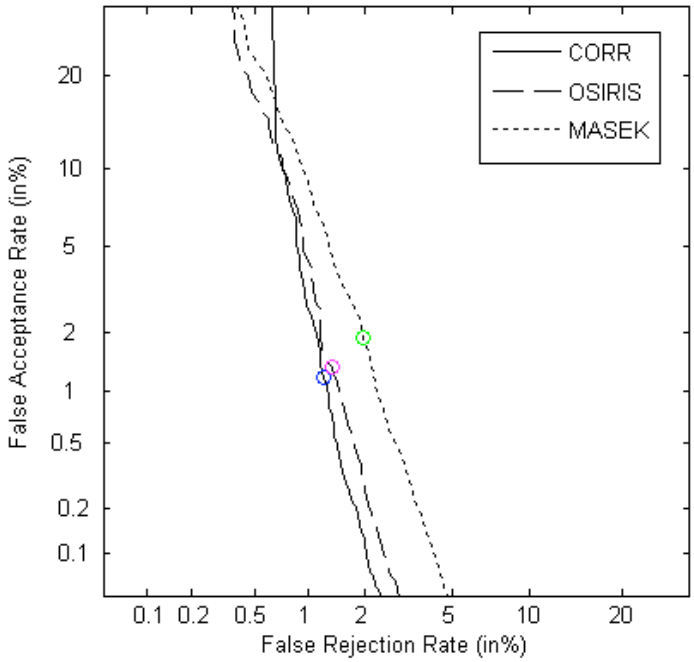

Fig.5 DET curves of CORR system (solid curve), OSIRIS system (dashed curve) and MASEK system (dotted curve) on ICE 2005 with the protocol of Experiment1.

2.1.2 Quality ranked comparative experiments

In order to quantify the robustness of our system to different levels of degradation, we performed a further study on ICE 2005 data. Indeed, the ICE 2005 database has been released with a global quality measure on each iris image, denoted by three different numbers: 3 (18 images), 4 (392 images) and 5 (1015 images), which correspond to respectively poor quality images, average quality images and good quality images. Because of the disparity in the number of images in the NIST subgroups, we have only considered two intra and inter comparison subsets of all the comparison resulting from Experiment1 using the NIST quality measure. In the first set (bad and average quality images), at least one image in the comparison is of quality 3 or 4. In the second set (good quality images), both images are of quality 5. Figure 6 shows the DET curves comparing OSIRIS, MASEK and CORR systems on two such quality-ranked subsets of the ICE 2005 protocol. Figure 6 shows that our system outperforms OSIRIS and MASEK on challenging conditions. Indeed, on bad and average quality subset (Fig.6(a)), CORR outperforms OSIRIS and MASEK independently of the functioning point. For example, at EER, CORR performance is 1.6%, OSIRIS 2.15% and MASEK 2.3%. Moreover considering the FRR at 0.1% of FAR, the improvement factor is even higher. This clearly shows the ability of our correlation-based approach to deal with degraded data.

Finally, on good quality data (Fig.6(b)), OSIRIS and CORR have similar performance around the EER functioning point, while OSIRIS is slightly better when low FAR values are considered (1.3% of FRR for OSIRIS and 1.6% of FRR for our system at 0.1% of FAR).

(a) (b)

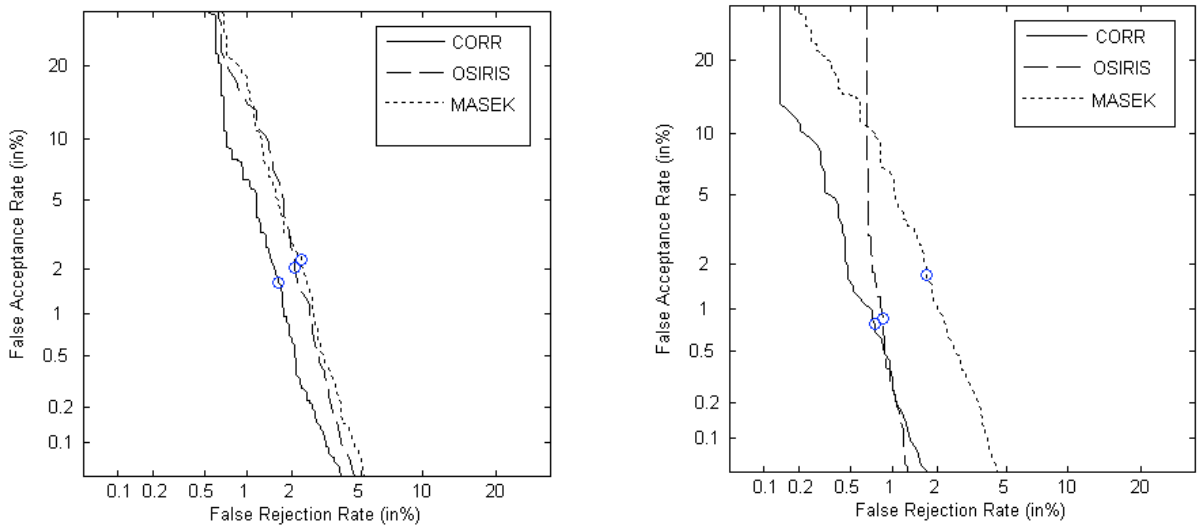

Fig.6 DET curves of CORR system (solid curve), OSIRIS system (dashed curve) and MASEK (dotted curve) on: (a) Bad and average quality subset (quality 3: 18 images and quality 4: 392 images), (b) Good quality subset (quality 5: 1015 images), of

ICE 2005 database and Experiment 1.

2.1.3 Comparative analysis on specific challenging degradations

In order to compare more precisely the behaviour of the two systems on degraded images, we also chose three different intraclass iris comparisons (test image vs. reference image) in which corrupted iris images are present. Such comparisons are shown in Figure 7, where in the top row are presented the reference images (a,b,c) while the corresponding test images are presented in the bottom row (d,e,f). In the first comparison (image (d) vs. image (a)), one can observe blurring on image (a). In the second comparison (image (e) vs. image (b)), a strong rotation is visible between the two images (roughly 20°). In the third comparison (image (f) vs. image (c)), there is a significant eyelid occlusion in the reference image (c).

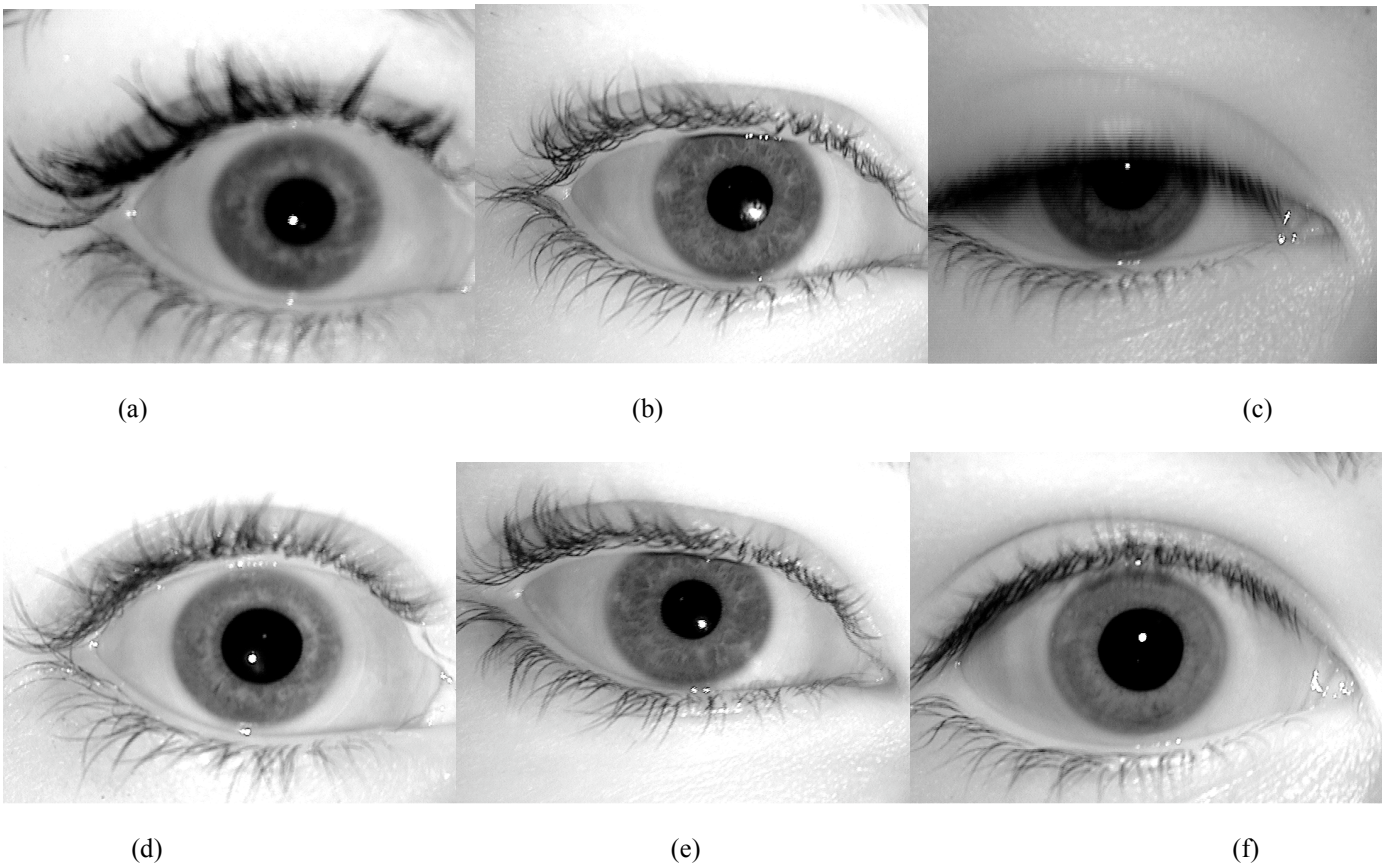

Fig.7 Three challenging intraclass comparisons from ICE 2005 database. The top row shows the reference images (a,b,c) while the corresponding test images are presented in the bottom row (d,e,f).

Figure 8 shows the interclass distributions of both OSIRIS and CORR systems' scores alongside the three intraclass distances obtained identified by A for the comparison of blurred image, B for the comparison of rotated image and C for the comparison of occluded image. We can see that in the two first comparisons, our

system handles without any problem blur and rotation effects, while OSIRIS fails to do so. Indeed, the scores generated by CORR on comparisons A and B are clearly far from the interclass distribution of CORR system's scores, while the distances generated by OSIRIS fall in the range of OSIRIS interclass distances. In the third comparison, neither OSIRIS nor CORR succeeded to overcome the huge eyelids occlusion. Indeed, this shows the limit of recognition approaches when there is not enough information available in the image.

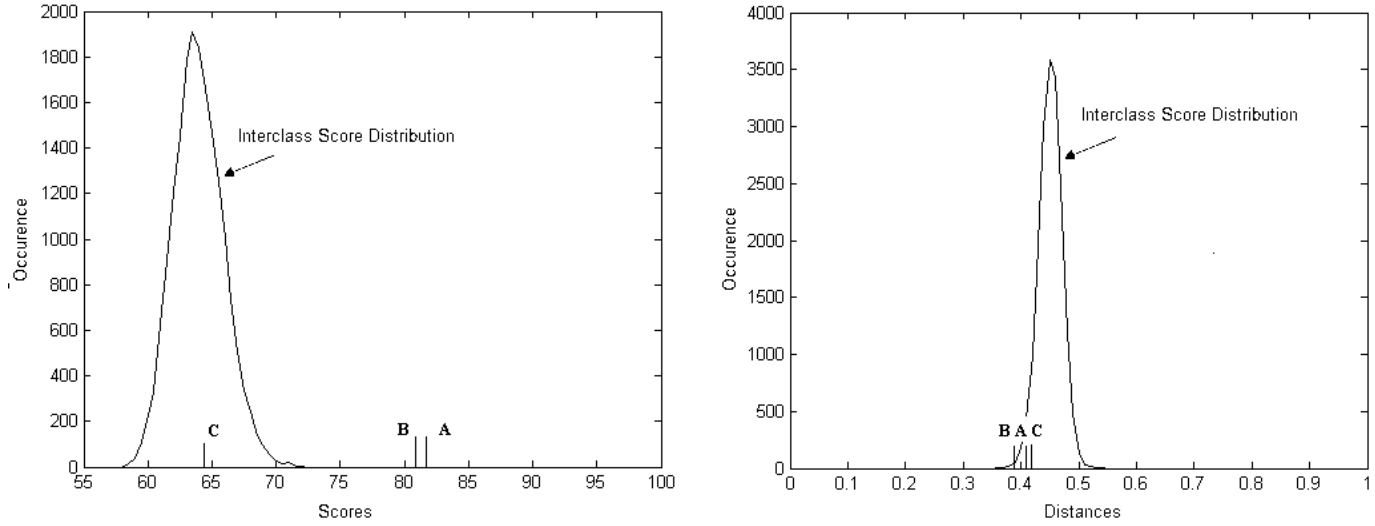

(a) (b)

Fig.8 Results of 3 challenging intraclass image comparisons (shown in Figure 7): mark **A** stands for comparison of images 7(d) v.s. 7(e), mark **B** stands for comparison of images 7(e) v.s. 7(b) and mark **C** stands for comparison of images 7(f) v.s. 7(c). Figure 8(a) shows results for CORR system and Figure 8(b) shows results for OSIRIS system.

We have confirmed these results when plotting the intraclass score distribution obtained by comparing good quality reference images (646 images) to each of the three categories of corrupted iris test images separately: blurred images (subset BL containing 639 images), rotated images (subset ROT containing 66 images) and occluded images (subset OCC containing 50 images). Indeed, as shown respectively in Figures 9, 10 and 11, the number of intraclass comparisons falling under the interclass distribution (zoomed for a better view) is very different for CORR and OSIRIS systems in the case of blur (32 for CORR and 111 for OSIRIS among 3035 comparisons, displayed in Figure 9) and rotated images (5 for CORR and 15 for OSIRIS among 256 comparisons, displayed in Figure 10). On the contrary, for occluded images, this number is similar (40 for CORR and 43 for OSIRIS among 189 comparisons, displayed in Figure 11).

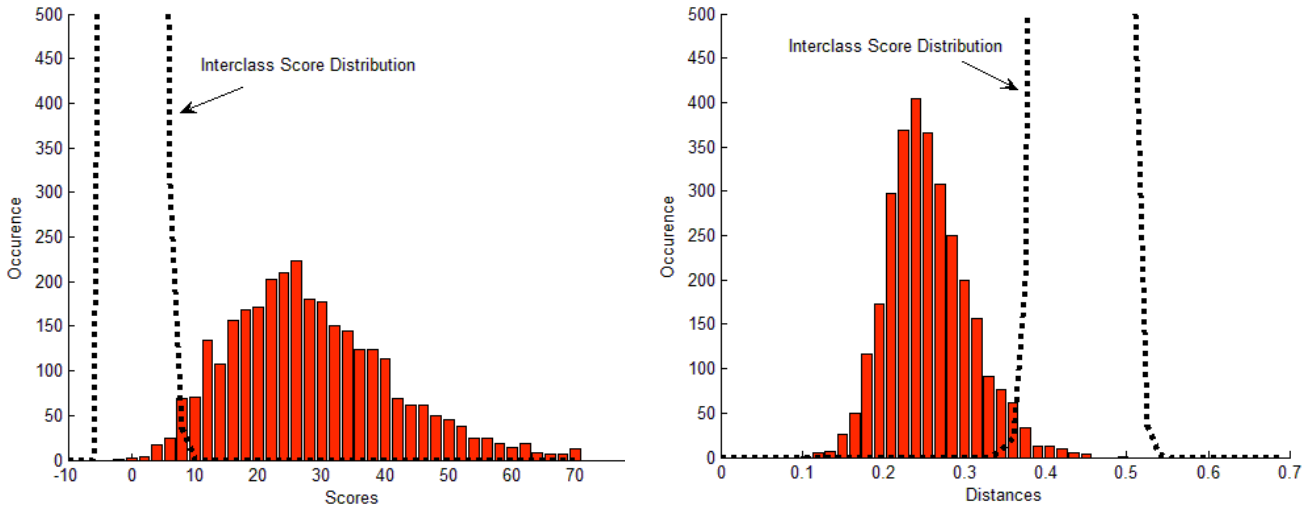

(a) (b)

Fig.9 Intraclass score distribution for CORR system on Fig. 9(a) and for OSIRIS system on Figure 9(b) when comparing good quality reference images with blurred test images (3035 comparisons). The interclass score distribution in each case is represented by a dashed line curve after zooming for a better view.

(a) (b)

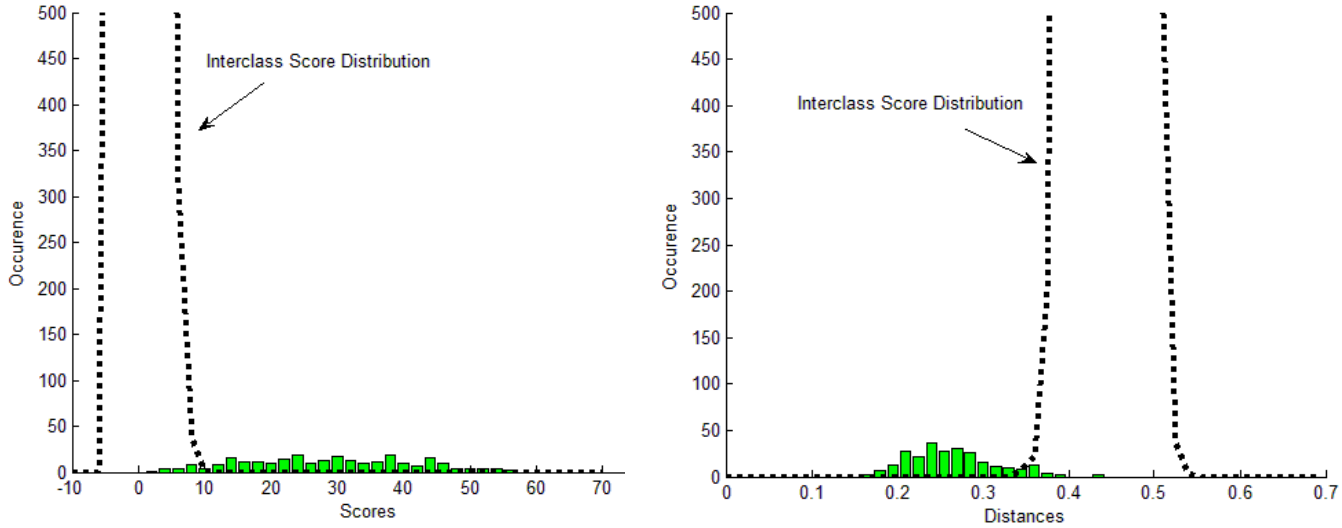

Fig.10 Intraclass score distribution for CORR system on Fig. 10(a) and for OSIRIS system on Figure 10(b) when comparing good quality reference images with rotated test images (256 comparisons). The interclass score distribution in each case is represented by a dashed line curve after zooming for a better view.

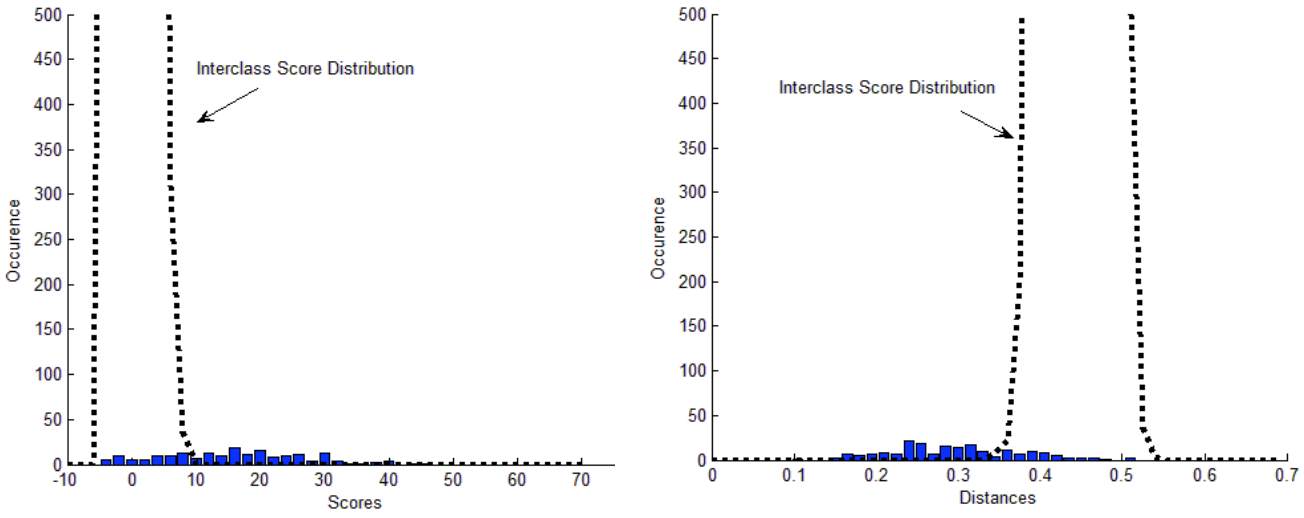

(a) (b)

Fig.11 Intraclass score distribution for CORR system on Fig. 11(a) and for OSIRIS system on Figure 11(b) when comparing good quality reference images with occluded test images (189 comparisons). The interclass score distribution in each case is represented by a dashed line curve after zooming for a better view.

2.2 Experiments on CBS

In the following, in order to compare our system (CORR) to OSIRIS and MASEK Reference Systems, we consider three different functioning points: the EER, the min(HTER) and the FRR at 0.1% of FAR. Table 1 shows comparative results on the two subsets (PATTEK and OKI sensors) in terms of HTER and FRR at 0.1% of FAR. Figure 12 shows some challenging images in the database (glasses, occlusion and blurring).

Roughly, on PATTEK data, our system outperforms OSIRIS by a factor 2, and by a quite important factor compared to MASEK results (sometimes between 10 and 20). On OKI data, our system still gives the best results but the improvement is not as important as with PATTEK sensor; indeed, on OKI data, a relative improvement of 25% is observed for CORR System compared to OSIRIS, and roughly by a factor 2 compared to MASEK. This phenomenon can be explained by the fact that, as shown in Figure 13, the iris images obtained with the PATTEK sensor are of less quality compared to those captured with the OKI sensor. This fact shows that our system is more robust to image degradations than the two Reference Systems. Indeed, the relative improvement brought by our approach compared for instance to OSIRIS is eight times higher on a subset of less quality (PATTEK sensor) than on the other subset of CBS database (OKI sensor). Once again, this result shows that our approach copes better with degradations than OSIRIS on this database.

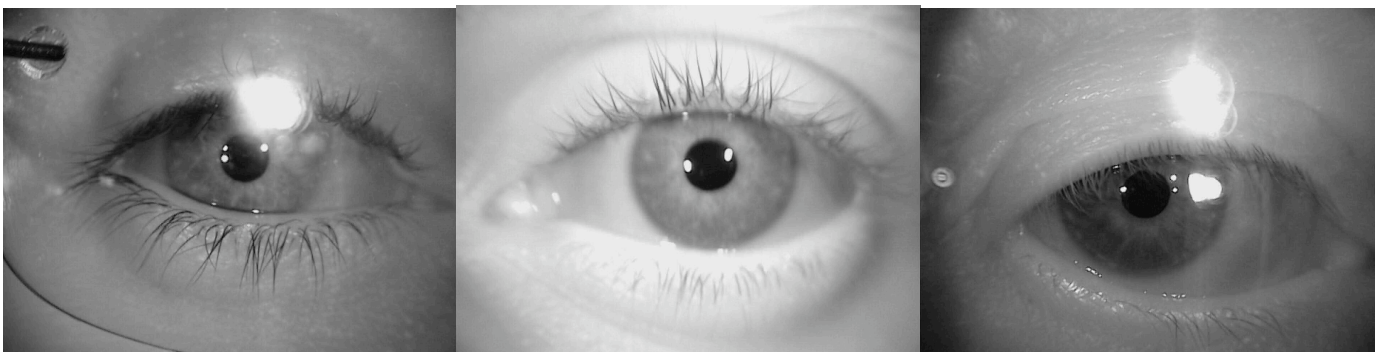

Fig. 12 Challenging images from CBS database (reflections due to glasses, blurring and occlusions).

		CORR		OSIRIS		Masek	
		1 Ref	3 Refs	1 Ref	3 Refs	1 Ref	3 Ref
CBS_Pattek	HTER	1.35%	1%	2.7%	1.9%	6.3%	4.3%
	FRR	3.2%	1.8%	6.2%	4%	54%	35%
CBS_OKI	HTER	1.5%	1%	2%	1.6%	4%	2.8%
	FRR	3%	2%	4.1%	3.2%	60%	5.2%

Tab1. Error rates at min(HTER) and FRR at 0.1% of FAR on CBS database (Pattek and OKI devices). Results are given using 1 sample as reference and also using 3 samples as reference.

Fig. 13 Images from CBS_OKI subset (left) and from CBS_PATTEK subset (right) of the same iris.

2.3 Complexity analysis

Although we have proven that our proposed method outperforms the two Reference Systems OSIRIS and MASEK in all cases in terms of error rates, an analysis in terms of template size and algorithm complexity must be done. First, the template size using an iris code-based method (such as OSIRIS) is equal to 256 Bytes, while our template size at this stage is equal to 15kBytes, that is roughly 60 times more. Nevertheless, even for a very large database (100 million references for example), this would require a storage capacity of 1.5 TBytes, largely

achievable with nowadays standards. The difficulty relies rather in algorithm complexity in the framework of large databases and performing subject identification. We have used in this work the fast cross Correlation-based method proposed by Lewis [24] for which the computation of all local correlations when comparing one reference image to one test image takes roughly 10^{-2} seconds on a 2.6 GHz PC. This allows performing 100 comparisons per second, that is 10.000 less comparisons than the Daugman approach on a 3GHz PC [5]. This comparison rate is reasonable for verification purposes in which only one-to-one comparison is performed, and is prohibitive for identification purposes on large databases with one standard PC platform. Nevertheless, many aspects of our algorithm are suited for parallelisation techniques. Indeed, we perform roughly one thousand local sub-image correlations for one comparison (test image vs. reference image) and these local correlations could be done in parallel.

IV. Conclusion

We have presented in this paper a novel phase correlation-based algorithm for iris authentication. Its originality relies on two aspects: the first one is the combination of local and global information extracted by the correlation measure and, the second one is the joint consideration of correlation peak amplitude and position in the matching score measured in a local manner.

We have considered the ICE 2005 database with the protocol of Experiment 1 in order to benchmark our system with state-of-the-art systems, in particular to other correlation-based systems, and to OSIRIS and MASEK Reference Systems. We start by showing that our recognition system outperforms these two systems using the same segmentation method and only adaptive histogram equalization pre-processing (no eyelids detection, no eyelashes removal …). This clearly shows the ability of our system to resist to degradations in images. Also, we have shown that our system is ranked among the first five systems (2% of FRR at 0.1% of FAR). Still, we must consider that such recognition approaches are not compared in equal conditions regarding since we did not perform prior sophisticated pre-processing contrary to most of the other systems in the evaluation.

We have also shown on quality-ranked subsets of the ICE 2005 database as well as on specific challenging cases how the proposed method resists to degradations in comparison to OSIRIS and MASEK, in particular to rotations and blurred images.

We have benchmarked our system in verification mode with OSIRIS and MASEK on CBS database that

contains the same proportion of European and Chinese subjects, as well as different degradations relatively to ICE 2005 database. The relative improvement brought by our approach compared to OSIRIS is eight times higher on a subset of less quality (PATTEK sensor) than on the other subset of CBS database (OKI sensor). Once again, this result shows that our approach copes better with degradations than OSIRIS on this database.

Future work will focus on an appropriate selection of sub-images for the local correlation process. Indeed, bad quality sub-images could be discarded from the local correlation process. This should also enhance our system's performance.

ACKNOWLEDGMENT

Portions of the research in this paper use the CASIA iris image database collected by Institute of Automation, Chinese Academy of Sciences as well as facilities of the NoE BioSecure

REFERENCES

[1] James R. Matey, Oleg Naroditsky, Keith Hanna, Ray Kolczynski, Dominick J. LoIacono, Shakuntala Mangru, Michael Tinker, Thomas M. Zappia, and Wenyi Y. Zhao, "Iris on the Move: Acquisition of Images for Iris Recognition in Less Constrained Environments", Proceedings of the IEEE, Vol. 94, No. 11, pp. 1936 – 1947, November 2006.

[2] John Daugman and Cathryn Downing, "Epigenetic randomness, complexity and singularity of human iris patterns". Proc. R. Soc Lond. B, Vol. 268, pp. 1737-1740, 2001.

[3] John Daugman, "High confidence Visual Recognition of Persons by a test of Statistical Independence", IEEE Transactions on Pattern Analysis and Machine Intelligence, Vol.15, No11, November 1993.

[4] John Daugman, "New methods in Iris Recognition", IEEE Transactions on Systems, Man, and Cybernetics, Part B, Vol. 37, N° 5, pp. 1167-1175, October 2007.

[5] John Daugman, "Probing the Uniqueness and Randomness of IrisCodes: Results From 200 Billion Iris Pair Comparisons", Proceedings of the IEEE, Volume 94**,** Issue 11, pp. 1927-1935, Nov. 2006.

[6] A. V. Oppenheim and J. S. Lim, "The importance of phase in signals", Proc. of the IEEE, Vol. 69, pp. 529-541, 1981.

[7] W.W. Boles and B. Boashash, "Human Identification Technique Using Images of the Iris and Wavelet Transform", IEEE Trans. Signal Processing, Vol. 46, No. 4, pp. 1185-1188, April 1998.

[8] John Daugman, "Flat ROC Curves, Steep Predictive Quality Metrics: Response to NISTIR-7440 and FRVT/ICE2006 Reports", http://www.cl.cam.ac.uk/~jgd1000/Response_2_NIST_7440.pdf, 2007.

[9] P. J. Philips "Test Director's ICE 2005 Presentation", http://iris.nist.gov/ICE/

[10] P. Jonathon Phillips, "FRGC and ICE Workshop", NRECA Conference Facility, March 22-23, 2006.

[11] P.J. Phillips, "FRVT 2006 and ICE 2006 Large-Scale Results," NIST Technical Report NISTIR 7408, 2007.

[12] CASIA Iris Images database, www.sinobiometrics.com.

[13] X. Li, "Modeling Intra-class Variation for Non ideal Iris recognition", International Conference on Biometrics, pp. 419-427, 2006.

[14] Y. Chen, S. C. Dass, A. Jain, "Localized Iris Image Quality Using 2D Wavelets", International Conference on Biometrics, pp. 387-381, 2006.

[15] S. A. C. Schuckers, N. A. Schmid, A. Abhyankar, V. Dorairaj, C. K. Boyce and L. A. Hornak, "On Techniques for Angle Compensation in Nonideal Iris Recognition", IEEE Transactions on Systems, Man, and Cybernetics- PartB, Vol. 37, No. 5, pp. 1176-1190, October 2007.

[16] John Daugman and Cathryn Downing, "Effect of Severe Image Compression on Iris Recognition Performance", IEEE Transactions on Information Forensics and Security, Vol. 3, N° 1, pp. 52-61, March 2008.

[17] R.P. Wildes, "Iris recognition: an emerging biometric technology", Proceedings of the IEEE, Vol. 85, N°9, pp. 1348-1363, September 1997.

[18] Jason Thornton, Marios Savvides and B.V.K Vijaya Kumar, "A Bayesian Approach to Deformed Pattern Matching of Iris Images", IEEE Transactions on Pattern Analysis and Machine Intelligence, Vol. 29, No 4, pp :596 – 606, April 2007.

[19] K. Miyazawa, K. Ito, H. Nakajima, "A phase-Based Iris Recognition Algorithm", International Conference in Biometrics, pp. 356-365, 2006.

[20] http://www.biosecure.info/

[21] Libor Masek, "Recognition of Human Iris Patterns for Biometric Identification" University of Western Australia, 2003.

[22] Aurelien Mayoue, "A Biometric Reference System for Iris, OSIRIS version 1.0", January 15th 2008. http://share.int-evry.fr/svnview-eph/

[23] D. Gabor, "Theory of communication", J. Inst Electrical Engineers, 1946.

[24] J. P. Lewis, "Fast Template Matching", Vision Interface, pp. 120-123, 1995.